NUCL SCI TECH (2017) 28:68
DOI 10.1007/s41365-017-0217-8

# A tracking system for the external target facility of CSR

Shu-Wen Tang[1] · Shi-Tao Wang[1] · Li-Min Duan[1] · Zhi-Yu Sun[1] · Yu-Hong Yu[1] · Xue-Heng Zhang[1] · Ke Yue[1] · Chen-Gui Lu[1] · He-Run Yang[1] · Peng Ma[1] · Fang Fang[1] · Duo Yan[1] · Yu Sun[1,2]

Received: 16 May 2016 / Revised: 26 September 2016 / Accepted: 27 September 2016 / Published online: 31 March 2017


**Abstract** A tracking system composed of three multi-wires proportional chambers (MWPCs) for the external target facility of the Cooler Storage Ring is reported in this paper. The active areas of the MWPCs are 518 mm × 400 mm, 582 mm × 450 mm, and 710 mm × 500 mm. Each MWPC consists of a series of alternately placed cathode and anode wire planes and can measure position along the directions of −30°, 0°, and 30° relative to horizontal. The construction and operation of the detectors are described, and a method for track reconstruction is introduced. A track-finding efficiency of about 62% and a spatial resolution of 1.21 mm have been achieved. The pion and proton can be identified clearly with the tracking system combined with a time-of-flight system.

**Keywords** ETF · MWPC · Track reconstruction · Spatial resolution

## 1 Introduction

One of the most interesting topics in nuclear physics is the research on the equation of state (EOS) of isospin asymmetric nuclear matter [1]. It has crucial significance for understanding some phenomenons from the structure of nuclei to the properties of massive stars. As the isovector part of the EOS, the density-dependent symmetry energy $E_{\mathrm{sym}}(\rho)$ is one of the most attractive and meaningful research points, but it is still very uncertain at high density, although many efforts were devoted during the past decades [2]. Reference [3] proposed several probes for determining $Esym(\rho)$ at high density experimentally. Among those probes, the $\pi^-/\pi^+$ ratio is the most sensitive one for beam energy near the pion production threshold [4], namely several hundred $A$ MeV.

An External Target Facility (ETF) has been constructed for CSR [5, 6] at Lanzhou. It delivers heavy-ion beams with energy up to 1$A$ GeV and is a very suitable place for study of $E_{\mathrm{sym}}(\rho)$ with the $\pi^-/\pi^+$ ratio as the probe, as well as for the study of the RIB physics [7]. The sketch of the experimental setup at ETF is shown in Fig. 1. The time of flight (TOF) of a charged particle is measured by the combination of a scintillator detector ($T_0$), placed upstream of the target, and a downstream scintillator wall (TOF wall) [8, 9], and the momentum of a charged particle is derived by a dipole magnet and the tracking system. The planar multiple wires chambers like MWPCs and MWDCs are good options for the tracking system mainly because of the advantages in low cost, large size, and the radiation resistance. From the considerations of performance and economy, the tracking system at ETF will be MWDCs at the final stage, and some work about the R&D of MWDC and the readout electronics are ongoing [10–13]. At the present stage, we choose MWPCs with highly integrated readout electronics as the tracking detectors for a pilot study. Two arms of the tracking system, each consisting of three MWPCs, and two TOF walls are placed at both sides

This work was supported by the National Natural Science Foundation of China (Nos. U1332207, 11222550, 11405242 and 11305222).

✉ Zhi-Yu Sun
sunzhy@impcas.ac.cn

1 Institute of Modern Physics, Chinese Academy of Sciences, Lanzhou 730000, China

2 University of Chinese Academy of Sciences, Beijing 100049, China

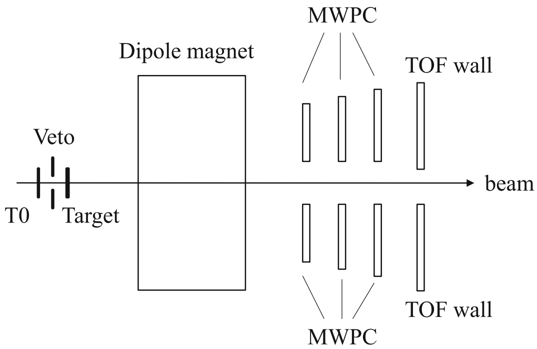


**Fig. 1** Sketch of the top view of the experiment setup at ETF

of the beam line to measure the positive- and negative-charged particles simultaneously.

During an EOS experiment, the beam and other heavy ions can be easily separated from pion with the magnetic field provided by the dipole, while the light particles, especially proton, are mixed together with pion due to the close magnetic rigidity. Therefore, the main task in the experiment is the $\pi$ and proton identification. As the tracking system is one of the key components for particle identification, high tracking efficiency and good spatial resolution are quite important. According to the result of a simulation with Geant4, the spatial resolution of the tracking system required for $\pi p$ identification should be better than several millimeters.

In this paper, the tracking system and its performance will be reported. The design and construction of the MWPC tracking detectors are described in Sect. 2. A testing experiment and some measurement results are presented in Sect. 3, and Sect. 4 is the conclusion.

## 2 Design and construction

The tracking system consists of three large area MWPCs in different sizes, as it is placed downstream the dipole magnet. Along the beam direction, the active areas of the MWPCs are 518 mm × 400 mm, 582 mm × 450 mm, and 710 mm × 500 mm, respectively. Each MWPC contains three anode planes of sense wires, named as $U$, $X$, and $V$. The $U$ and $V$ wires are inclined by the degree of 30° and −30° with respect to the vertical $X$ wires. Each of the anode planes is sandwiched in two cathode planes, and the distance between every adjacent plane is 5 mm. The anode planes consist of parallelly arranged gold-plated tungsten wires in diameter of 25 μm. The multiple scattering effect of a light particle in air is quite noteworthy, and a diffusion of about 1.2 mm is estimated for the 500 MeV/c pion after 1 m transportation. Therefore, the detectors should be placed compactly to reduce the negative effect of the multiple scattering as much as possible. The minimum transportation distance is 3 m, and the diffusion caused by multiple scattering is as much as 3.6 mm. Therefore, a few millimeters spatial resolution is enough for a pilot study. As a result, the sense wires are determined to have a 4-mm spacing for $X$ planes and have a 6-mm spacing for $U$ and $V$ planes. The cathode wires are made of beryllium copper in diameter of 75 μm with 1 mm spacing. All the wires are positioned and tensed with a programmable winding machine. The positioning accuracy of the wires is about 25 μm, and the tension provided on the anode wires is 70 g, and on the cathode wires, it is 200 g. The main parameters for the three types of MWPCs are listed in Table 1. The three MWPCs have been assembled and installed at ETF, and Fig. 2 shows them used in a testing experiment.

The PCOS4 electronics [14] manufactured by the LeCroy Corporation are used as the readout electronics for the MWPCs. The electronics contain three basic components, which are 2741 chamber mounted cards, custom-made backplanes, and two CAMAC modules. Each 2741 card (FE board) contains four MQS104 preamplifier chips and two MDL108 chips for delay and coincidence and can provide readout for 16 MWPC wires. As a result, 64 2741 cards are needed in total for all the three MWPCs. Four streams in different backplanes combine data from the 2741 cards and send it to a CAMAC module 2748CAM and feed back the control information. All data are first encoded and stored in the 2748 module, and then transferred to the DAQ system. Another CAMAC module 2749CAM communicates with the experiment's trigger system and coordinates the 2748 stream controller. The main advantage of the PCOS4 electronics is high integration and simplicity to use. The information is recorded wire by wire, and the threshold can be set for groups of four wires, while the delays can be set for each wire individually.

## 3 Testing experiment

The tracking system has been tested at ETF in an experiment of a 600 MeV/u $^{12}C$ beam bombarding a $^{12}C$ target. The operation of the detectors and a data analysis method will be introduced, and some results will be presented below.

### 3.1 Operation and performance

The chambers were operated in proportional mode with the gas mixture of 80% argon and 20% carbon dioxide at room temperature and atmospheric pressure. The positive high voltage was applied to the anodes, while the cathodes were grounded. Considering the balance between the discharge probability and the detection efficiency during the

**Table 1** Main parameters for the MWPCs

| | MWPC$_1$ | | | MWPC$_2$ | | | MWPC$_3$ | | |
|---|---|---|---|---|---|---|---|---|---|
| Active area (mm$^2$) | 518 × 400 | | | 582 × 450 | | | 710 × 500 | | |
| Cathode wire Φ | Be–Cu 75 μm | | | Be–Cu 75 μm | | | Be–Cu 75 μm | | |
| Cathode wire spacing (mm) | 1 | | | 1 | | | 1 | | |
| Sense wire Φ | Au–W 25 μm | | | Au–W 25 μm | | | Au–W 25 μm | | |
| | *U* | *X* | *V* | *U* | *X* | *V* | *U* | *X* | *V* |
| Number of sense wires | 80 | 128 | 80 | 96 | 144 | 96 | 112 | 176 | 112 |
| Number of FE boards | 5 | 8 | 5 | 6 | 9 | 6 | 7 | 11 | 7 |
| Sense wire spacing (mm) | 6 | 4 | 6 | 6 | 4 | 6 | 6 | 4 | 6 |

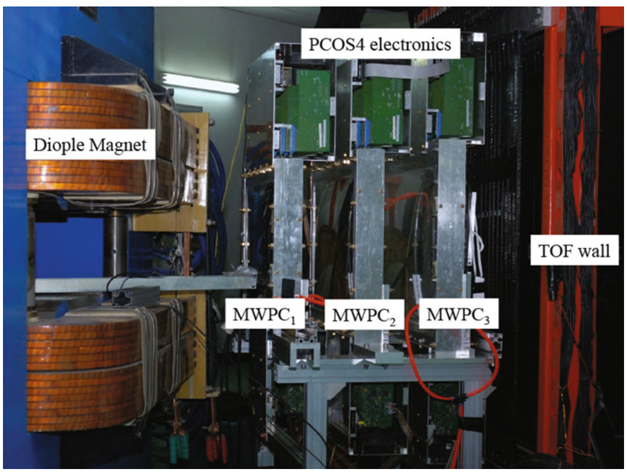


**Fig. 2** (Color online) The experimental setup at ETF. Three MWPCs were assembled and tested at ETF

actual experimental runs, the anode voltage in *X* planes was set at 2200 V, and it was set at 1930 V in *U* and *V* planes. The threshold of each FE board was carefully set according to the multiplicity of hit wires. The principle was making sure that the number of wires hit by a charged particle was as less as possible on the premise of high detection efficiency. The multiplicity of hit wires in every plane of the MWPCs is plotted in Fig. 3. In most of the events, the multiplicities for all the MWPC planes were one or two. In some events, the multiplicity was a little bit higher than two and it was caused by the big incident angle. Meanwhile, in few events the multiplicity was quite large, implying that slight discharge existed. The detection efficiencies for all the wire planes are listed in Table 2. The way to calculate the detection efficiency was that the number of events detected by the wire plane divided by the number of events for particles crossing the plane. For all the wire planes, the detection efficiencies were nearly higher than 95%.

### 3.2 Track reconstruction

The wires fired by a charged particle crossing the MWPCs distributed in many wire planes, and each plane gave spatial information in one coordinate. The track could be reconstructed by combining the information of all the planes. The track-finding algorithm was based on a three-stage procedure as following:

The first step was to select the candidate hit wires in each wire plane. It was done separately by groups of *U*, *X*, and *V* among the three MWPCs. In each group, only hit wires in three MWPC planes matching a straight line were considered as valid hit wires, and other combinations were forbidden. Figure 4a shows an example of selecting the hit wires.

The second step was to select the candidate combinations of hit wires in *U*, *X*, and *V* planes and was done in each MWPC. As an example, shown in Fig. 4b, all the candidate wires in the MWPC planes were projected on the same vertical plane, and each combination of three lines in different planes delimited a triangle. As the incident angles of the charged particles were very small, the area of the triangle corresponding to good solution had to be small. An upper limit of the area, $s_0$, was applied in the procedure. Only the solution with the area smaller than $s_0$ was allowed.

The last step, shown in Fig. 4c, was fitting the tracks with the selected triangle wires. Accordingly a valid track was a straight line and that the sum of the squared distances to all the 9 candidate wires had to be smaller than a given upper limit value, and the positions in each MWPC could be calculated. Therefore, the deviation between the calculated position and the measured position (the position of hit wire) could be obtained, and the result in the *x* direction is shown in Fig. 5. The spatial resolution was $\sigma$ = 1.21 mm, which was consistent with the theoretical value $4/\sqrt{12}$=1.15 mm.

As the track-finding method described above, only a charged particle detected by all the 9 anode planes of the

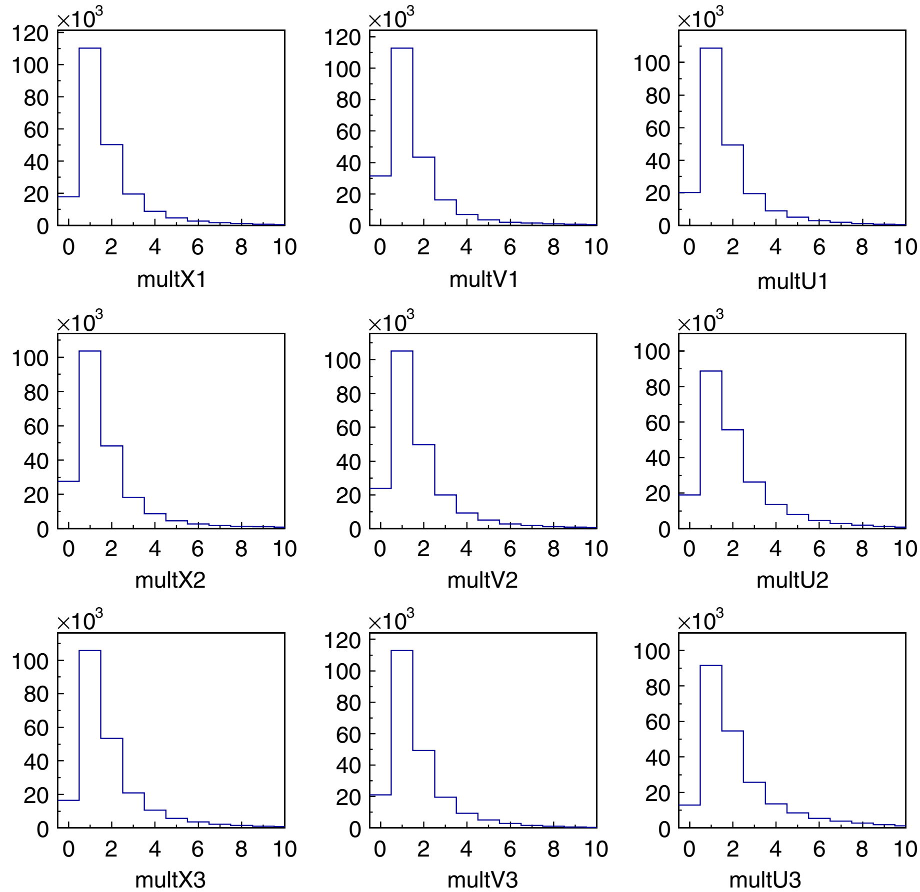


**Fig. 3** The multiplicity of hit wires in the MWPC planes

**Table 2** Detection efficiencies for the MWPC wire planes

| | *U* (%) | *X* (%) | *V* (%) |
|---|---|---|---|
| $MWPC_1$ | 95.6 | 97.7 | 94.5 |
| $MWPC_2$ | 96.4 | 96.0 | 96.0 |
| $MWPC_3$ | 96.1 | 95.7 | 95.2 |

MWPCs can reconstruct a successful track. Figure 6 shows the number of tracks reconstructed per event during a typical experimental run. About 38% of the events reconstructed no tracks because of the missing efficiency in some of the anodes. In 54% of the events, there was only one track, and two track events accounted for about 6%. The higher number of tracks events maybe mis-reconstructed due to the discharge. The track reconstruction efficiency was about 62%. If we determine a candidate track with a combination of hit wires in less than three detection planes of each chamber, the track reconstruction efficiency can be improved at the cost of worse spatial resolution. It is a balance between efficiency and resolution.

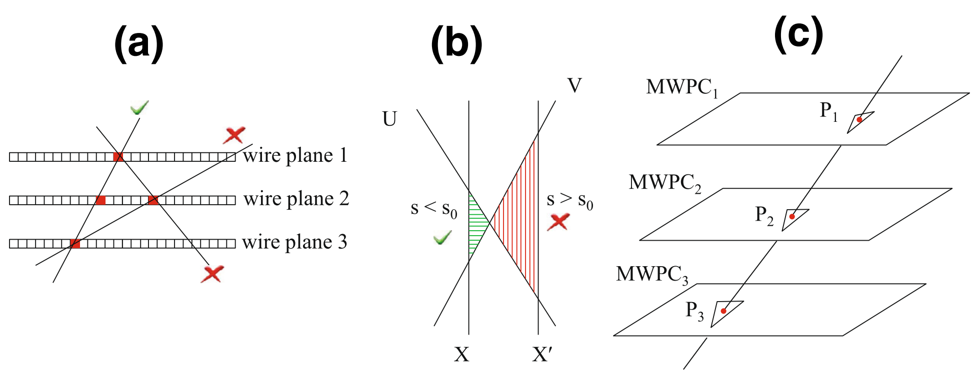


**Fig. 4** (Color online) The three-stage procedure for track reconstruction. **a** Hit wires recognition. **b** Combinations of wires determination in one MWPC. **c** The track fitting

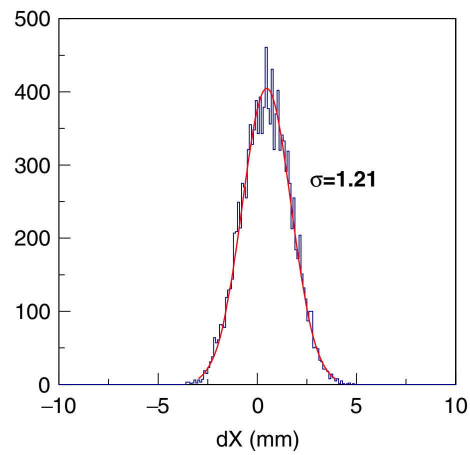


**Fig. 5** (Color online) Deviation between the calculated position and the hit wire in the $x$ direction

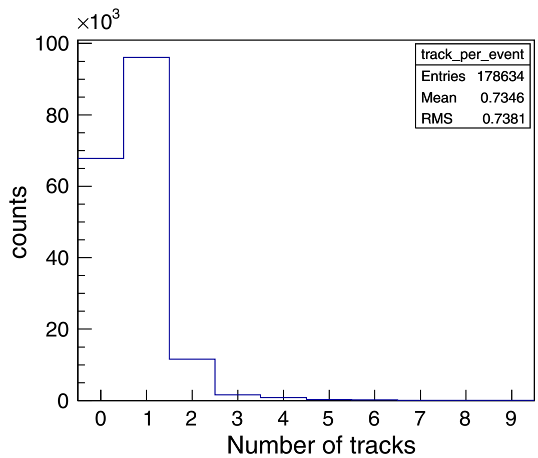


**Fig. 6** Number of tracks reconstructed per event during a typical experimental run

### 3.3 Particle identification

The reconstructed tracks were extrapolated to the TOF wall and matched with the positions of fired strips. If the track crossed the proper strip or the deviation was tolerant, then the track was accepted. Since the detection efficiency of the TOF wall was almost 100%, most of the track matchings were successfully established. For such events, the trajectories of the charged particles were reconstructed with a simple magnetic field model: The magnetic field in the dipole was uniform, while outside the dipole it was negligible. Then the momentum was calculated with the track length in the dipole multiplied by the magnetic field strength. The velocity of a charged particle can be derived from the TOF information and the total track length from the $T_0$ detector to the TOF wall, which eventually led to reconstruction of the mass of the particle. The momentum information and the particle mass can be used for particle identification (shown in Fig. 7). Although the reconstruction method was not fine enough to consider the magnetic field outside the dipole, the products of $\pi^+$, $\pi^-$, and proton could be identified clearly. The reconstructed mass in Fig. 7, varying with the momentum, was caused by the systematic deviation of the TOF calibration and the resolutions from time and position.

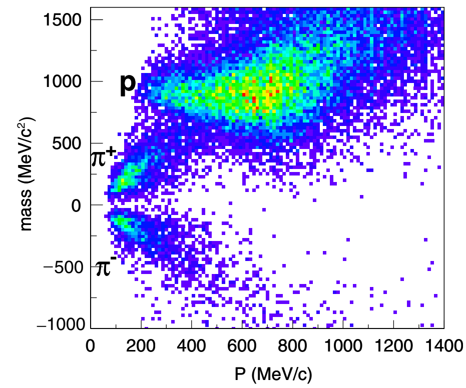


**Fig. 7** (Color online) Particle identification of $\pi^+$, $\pi^-$, and proton

## 4 Conclusion

The tracking system including three large area MWPCs was set up at the ETF of CSR for the study of EOS of isospin asymmetric nuclear matter. Each MWPC contained three anode wire planes whose wires were inclined by the degree of $-30°$, $0°$, and $30°$ relative to vertical. The chambers were operated with 80% Ar and 20% $CO_2$ at room temperature and atmospheric pressure and were read out by the PCOS4 electronics. A detection efficiency of over 95% for all the anode planes was achieved under the given working voltage. A three-stage algorithm was introduced for the track reconstruction. A spatial resolution of 1.21 mm and the track-finding efficiency of about 62% could be achieved. The tracking system was used in some testing experiments and had been proven to own the ability to identify pion and proton easily. In a word, the tracking system can meet the demand of the EOS experiment.

## References

1. M. Di Toro, V. Baran, M. Colonna et al., Probing the nuclear symmetry energy with heavy-ion collisions. J. Phys. G: Nucl. Part Phys. **37**, 083101 (2010). doi:10.1088/0954-3899/37/8/083101
2. Z.G. Xiao, G.C. Yong, L.W. Chen et al., Probing nuclear symmetry energy at high densities using pion, kaon, eta and photon productions in heavy-ion collisions. Eur. Phys. J. A **50**, 37 (2014). doi:10.1140/epja/i2014-14037-6

3. B.A. Li, L.W. Chen, C.M. Ko, Recent progress and new challenges in isospin physics with heavy-ion reactions. Phys. Rep. **464**, 113–281 (2008). doi:10.1016/j.physrep.2008.04.005
4. Z.G. Xiao, B.A. Li, L.W. Chen et al., Circumstantial evidence for a soft nuclear symmetry energy at suprasaturation densities. Phys. Rev. Lett. **102**, 062502 (2009). doi:10.1103/PhysRevLett.102.062502
5. J.W. Xia, W.L. Zhan, B.W. Wei et al., The heavy ion cooler-storage-ring project (HIRFL-CSR) at Lanzhou. Nucl. Instrum. Methods A **488**, 11–25 (2002). doi:10.1016/S0168-9002(02)00475-8
6. J.W. Xia, Y.J. Yuan, Y. Liu et al., HIRFL-CSR commissioning in 2006 and 2007. Chin. Phys. C **33**, 12–17 (2009). doi:10.1088/1674-1137/33/S2/004
7. K.A. Li, Y.L. Ye, Recent development in experimental RIB physics. Nuclear Technol. **37**, 100501 (2014). doi:10.11889/j.0253-3219.2014.hjs.37.100501 (**in Chinese**)
8. Y.H. Yu, H.G. Xu, H.S. Xu et al., Studies of timing properties for a TOF counter at an external target facility. Chin. Phys. C **33**, 781–784 (2009). doi:10.1088/1674-1137/33/9/014
9. Y.J. Zhang, Y.H. Yu, Y. Zhou et al., Development of a test bench for plastic scintillator counters for the DAMPE. Nucl. Technol. **38**, 080403 (2016). doi:10.11889/j.0253-3219.2015.hjs.38.080403 (**in Chinese**)
10. H. Yi, Z. Zhang, Z.G. Xiao et al., Prototype studies on the forward MWDC tracking array of the external target experiment at HIRFL-CSR. Chin. Phys. C **38**, 126002 (2014). doi:10.1088/1674-1137/38/12/126002
11. W.J. Cheng, Z. Zhang, H. Yi et al., Development of a fan-in and delay module for MWDC based on Flash-ADC acquisition scheme. Nuclear Technol. **39**, 040403 (2016). doi:10.11889/j.0253-3219.2016.hjs.39.040403
12. H. Li, S. Zhang, F. Lu et al., Simulation of momentum resolution of the CEE-TPC in HIRFL. Nuclear Technol. **39**, 070401 (2016). doi:10.11889/j.0253-3219.2016.hjs.39.070401 (**in Chinese**)
13. L.F. Kang, L. Zhao, J.W. Zhou et al., A 128-channel high precision time measurement module. Metrol. Meas. Syst. **20**, 275–286 (2013). doi:10.2478/mms-2013-0024
14. PCOS 4 System Manual. http://cdn.teledynelecroy.com/files/manuals/pcos4man.pdf